PHYSICAL REVIEW E **67**, 040701(R) (2003)

Continuous isotropic-nematic liquid crystalline transition of *F*-actin solutions

Jorge Viamontes and Jay X. Tang*
Physics Department, Brown University, 184 Hope Street, Providence, Rhode Island 02912
(Received 4 September 2002; published 8 April 2003)

The phase transition from the isotropic (*I*) to nematic (*N*) liquid crystalline suspension of *F*-actin of average length $l \geqslant 3$ μm was studied by local measurements of optical birefringence and protein concentration. Both parameters were detected to be continuous in the transition region, suggesting that the *I*-*N* transition is higher than first order. Thus we report experimental evidence for a continuous *I*-*N* transition for a suspension of rodlike macromolecules. Our findings are consistent with a recent theory by Lammert, Rokhsar, and Toner [Phys. Rev. Lett. **70**, 1650 (1993)], predicting that the *I*-*N* transition may become continuous due to suppression of disclinations.

DOI: 10.1103/PhysRevE.67.040701 PACS number(s): 61.30.Eb, 61.30.Jf, 64.70.Md, 82.35.Pq

The isotropic (*I*) to nematic (*N*) liquid crystalline transition occurs in solutions of rodlike particles including stiff polymers [1], protein filaments [2,3], and filamentous viruses [4]. These macromolecules are charged in aqueous solutions and interact with each other only by a short-ranged repulsion (the Debye screening length is typically on the order of a nanometer) due to thermal collisions. The short range repulsion and the noninterpenetrability of the macromolecules together define the excluded volume effect, which causes the nematic formation in order to maximize the translational entropy and thus minimize the free energy of such systems at sufficiently high concentrations. The transition of this nature is predicted to be first order based on a statistical mechanical theory by Onsager in 1949 [5]. One explicit parameter in the free energy expression for the rodlike suspension is the concentration of macromolecules c rather than temperature T for analyzing the *I*-*N* transition of thermotropic nematogens [6]. However, both systems have the same nematic order parameter $S = \int d\Omega f(\theta) P_2(\theta)$, where $f(\theta)$ is the orientational distribution function and $P_2(\theta) = [3\cos^2(\theta) - 1]/2$ is the second Legendre polynomial. Landau and de Gennes [7] treated the *I*-*N* transition by a general method of free energy expansion as a function of S, which contains a third order term and thus predicts the *I*-*N* transition to be of first order. This classic analysis led to the conventional wisdom that the *I*-*N* transition belongs to a different universality class than the magnetic systems. In the magnetic systems the magnetization, a vector, is the order parameter. All odd powers of the order parameter are forbidden in the energy expansion, and thus the order-disorder transition is generally continuous.

In a recent theory examining topology and nematic ordering by Lammert, Rokhsar, and Toner (LRT) [8], it is shown, however, that the weakly first order *I*-*N* transition can break into two continuous transitions if the disclination core energy is raised sufficiently high. No particular experimental system has been shown to date in direct support of the theory. In this Rapid Communication, we present experimental features of the *I*-*N* transition of *F*-actin, and then discuss the relevance of our surprising findings to the theory of LRT.

The protein filaments *F*-actin provide us a challenging system to study the liquid crystalline transition. On one hand, since the protein is well characterized biochemically, special techniques such as fluorescence labeling are available to probe both structure and dynamics of an *F*-actin solution [9]. On the other hand, extreme polydispersity in filament length due to the stochastic nature of actin polymerization renders the theoretical analysis of the *I*-*N* transition less definitive than for the simpler monodisperse systems. Recent experimental studies show that *F*-actin forms a nematic phase at a concentration slightly above 2 mg/ml [3,10–12]. The onset actin concentration for the *I*-*N* transition is inversely proportional to the average filament length l [10,12]. There have also been bulk measurements suggesting a concentration range, in which partially aligned domains exist [12]. The initial goal of our study was to determine the *I*-*N* transition phase diagram by measuring local alignment of *F*-actin, the coexisting *I*-*N* domains, and the variation of local protein concentrations c. Through these measurements, we discovered surprising features suggesting that the *I*-*N* transition of *F*-actin is continuous.

For a sample of an aligned array of rodlike filaments, the difference in index of refraction between the direction of the alignment and the direction perpendicular to it can be measured optically. This difference, known as the optical birefringence, Δn, is directly proportional to the order parameter of a nematic suspension S. In this Rapid Communication, the birefringence measurements were performed on a Nikon TE-300 microscope, equipped with a Cambridge Research Inc. (CRI) Polscope package (Cambridge, MA). The Polscope software is capable of determining local retardance, $\Delta d = \Delta n d$, where d is the sample thickness, as well as the directions of slow axis throughout the sample [13]. The measured retardance by the Polscope can also be averaged over all pixel values for the entire field of view. This avoids the cancellation effect due to different alignment directions of different domains.

We used the Polscope technique to measure Δd of *F*-actin over a range of concentrations and several average filament lengths l regulated by adding calculated, trace amounts of nucleating and filament severing protein called gelsolin. This method of regulating l has been well established in actin biochemistry, and was used in the previous *I*-*N* transition

*Email address: physics.brown.edu

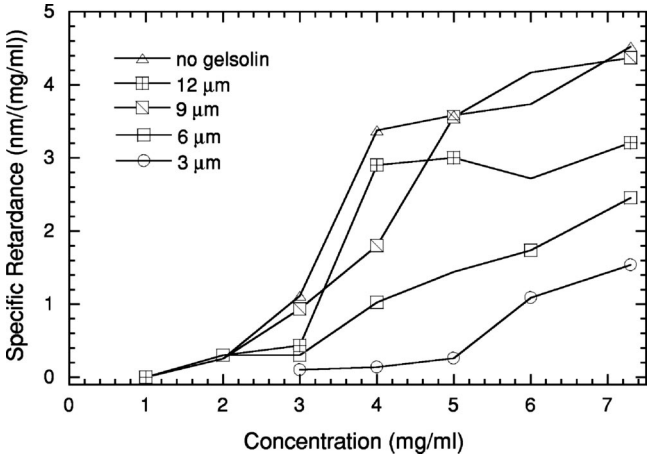

FIG. 1. Average specific retardance, $\Delta d/c$, plotted for *F*-actin in the concentration range of 1.0–7.3 mg/ml, and of five different ℓ. The data show the region of *I*-*N* transition for *F*-actin.

studies of *F*-actin [10,12]. We used rectangular capillary tubes of 0.4 mm thickness and 8 mm width to make aligned *F*-actin samples. After injecting an actin solution of the desired concentration into the capillary tube immediately following the addition of 50 mM KCl and 2 mM $MgCl_2$ to start polymerization, both ends were sealed with melted plastic. The sample was aligned by upside down inversions using a table top centrifuge. Repeated spins showed that the average birefringence of the sample reached a saturation value after two or three inversions (data not shown). Figure 1 shows $\Delta d/c$ as a function of c and ℓ. The selected results shown in Fig. 1 confirm the previous findings that the threshold concentration of the *I*-*N* transition is inversely related to ℓ [10,12]. The specific retardance, $\Delta d/c$, increases with c and reaches a saturated level at $\ell \geqslant 9$ μm. Further increase in c increased Δd, but not $\Delta d/c$, suggesting that the entire sample was in the nematic state. Actin samples of shorter ℓ did not reach the saturation level for $\Delta d/c$, suggesting that either the filaments were only weakly aligned, or that the measured value was the weighed average of coexisting domains. Variation of retardance was observed, but usually over relatively large regions with no sharp boundaries. No clearly separated domains of either *I* or *N* phase were detected based on the retardance measurements.

The basic criterion for a first order phase transition of a rodlike suspension is that coexisting *I*-*N* domains are expected, which contain filaments of different concentrations. In order to detect the concentration difference between coexisting *I*-*N* domains of *F*-actin, TRITC- phalloidin (Sigma, St. Louis, MO) was added in a ratio of 1 dye molecule per 1000 actin monomers. Phalloidin is a tiny molecule that binds to *F*-actin tightly. Despite the submicromolar concentration, the molecular density of the dye attached to *F*-actin was on the order of 100 per μm^3. Due to the random binding of phalloidin to *F*-actin, the intensity of fluorescence is proportional to the concentration of actin. Therefore, fluorescence imaging provides us a quantitative report of concentration variation down to the scale of microns. This technique is especially valuable as one examines regions of the sample where local birefringence varies. Measurements of retardance and fluorescence were performed for a number of *F*-actin samples in order to correlate variations of both parameters. Figure 2 displays both measurements at exactly the same location in one representative condition of a 7.3 mg/ml *F*-actin sample of $\ell = 3$ μm. It is shown in Fig. 1 that *F*-actin under this condition is in the *I*-*N* transition region. Therefore, one would expect to have *I*-*N* co-existence based on the theoretical predictions of a first-order transition. We see in Fig. 2(a) a continuous variation in both Δd and direction of the slow axis over the region, showing alternating stripes of high and low values. Such a zebra pattern with white stripes and black grooves appeared occasionally in thick samples, as well, a phenomenon reported previously by others [10,12]. The most surprising result here is that the corresponding fluorescence image [Figs. 2(c) and 2(d)] shows constant c over the entire region of this sample. Therefore, the white stripes and black grooves are not coexisting *N*-*I* domains.

In most of our observations for the nematic samples of $\ell \geqslant 3$ μm, zebra patterns were either not formed, or too fuzzy to be discerned. Instead, the birefringence pictures appeared rather uniform (data not shown). The same result of uniform concentration holds for weakly birefringent regions of less defined patterns, as well. In all actin concentrations up to 7.3 mg/ml and $\ell \geqslant 3$ μm, we saw no discernable domain boundaries of coexistence based on the retardance data. Instead, a blending of domains of comparable levels of alignment was occasionally observed, which led to either zebra patterns or other variants. Throughout all samples tested c was measured to be uniform, forcing us to conclude that no coexistence occurred to *F*-actin spanning the region of *I*-*N* transition.

Additional experiments were performed to examine two possible causes for the lack of concentration variation in the *I*-*N* transition of *F*-actin. First, we suspected that the *F*-actin network might be weakly crosslinked [15]. As a result, the polymerizing actin solution may first form a nematic phase when ℓ reaches the value required by the excluded volume effect. Further polymerization and/or annealing by even a weak crosslinking effect may lead to gelation so that the network is unable to achieve thermodynamic equilibrium with well separated *I*-*N* domains in coexistence. A second possibility is that the extremely long *F*-actin tends to get sufficiently entangled and thus kinetically trapped in a gel-like or glassy state with local orientational order but no global phase equilibrium. To address these concerns, we mixed a small number of labeled filaments with 7.3 mg/ml unlabeled *F*-actin, both of $\ell = 3$ μm, and observed thermal motions of the labeled filaments. We found that the filaments diffuse rapidly and preferentially along their axis. The diffusion coefficient of each labeled filament was determined by calculating the $\langle \Delta x^2 \rangle$ over a movie sequence of 50–150 frames. The translational diffusion of labeled filament along its axis was determined to be $D_{\|} = 1.30/L$ (μm^2/sec), where L, omitting its unit of μm, is the length of the diffusing filament. The prefactor of 1.30 was obtained from the fit to a large number of measured values of various filament lengths (data not shown). For comparison, the measured values were about 1/3 of the values we measured for the diffusion coefficient of *F*-actin confined in a thin layer and in the dilute limit. This reduction by a factor of 3 is not surprising, since

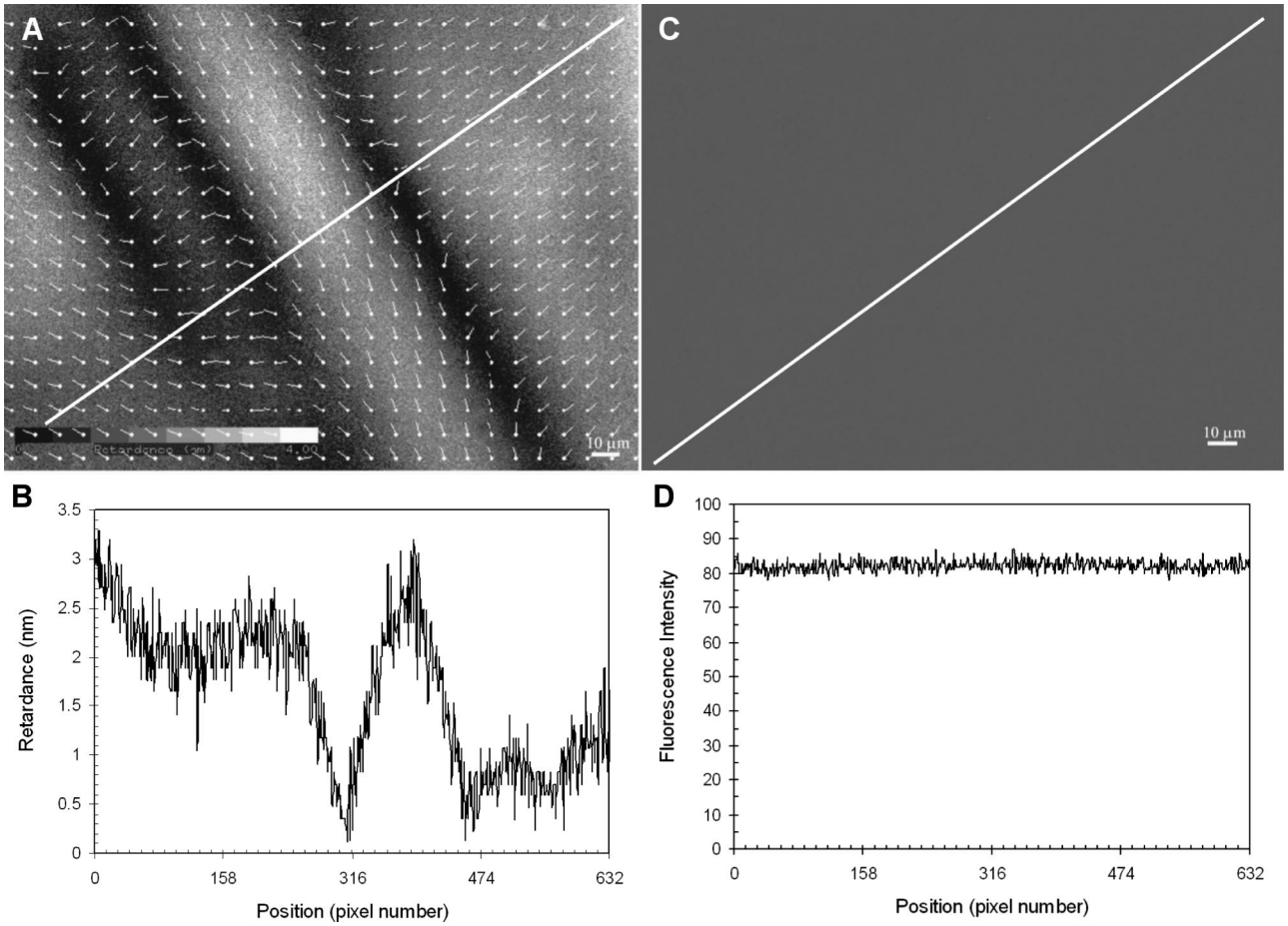

FIG. 2. (a) Retardance values of 7.3 mg/ml *F*-actin with $\ell = 3\ \mu$m. The gray scale of 0–4 nm covers the range of Δd. (b) A line plot of Δd along the diagonal cut, shown from the top right to the bottom left. (c) Fluorescence image of the same region. The measured intensity values varied from 82 to 85 only, over the camera range of 0–255. (d) A line plot diagonally across the image, showing little variation in intensity value. The sample thickness is 10 μm.

F-actin is highly entangled at a few mg/ml. In contrast, the lateral and rotational diffusion coefficients are suppressed by factors of at least 10 and 100, respectively, estimated based on the same analysis.

We propose that the *I*-*N* transition of *F*-actin of $\ell \geqslant 3\ \mu$m corresponds to the continuous transition between a topologically ordered isotropic phase (*T*) and a weakly aligned nematic phase (*N*), as predicted theoretically by Lammert, Rokhsar, and Toner (LRT) [8]. First, the suspension of long (aspect ratio over 300) and stiff (persistence length 15-20 μm [17]) *F*-actin satisfies one key criterion of defect suppression, which according to the LRT theory renders the transition continuous. The disclination lines are energetically costly for *F*-actin, as the bending elastic constant (K_3) is far greater than splay (K_1) and twist (K_2) for long and stiff rods [16]. Indeed, few line defects and nearly no disclinations were observed in *F*-actin samples. We note that the black grooves in Fig. 2(a) are not disclination lines [14]. Second, suppression of rotational diffusion likely prevents long filaments from flipping in the concentrated *F*-actin. Therefore, vectorial directions can be assigned to individual filaments, and in this context, the isotropic state becomes topologically ordered.

A schematic phase diagram for *F*-actin is shown in Fig. 3, which translates the main predictions of the LRT theory, as depicted in Fig. 2 of Ref. [8]. Note that the LRT theory has been developed in analogy to the ferromagnetic-

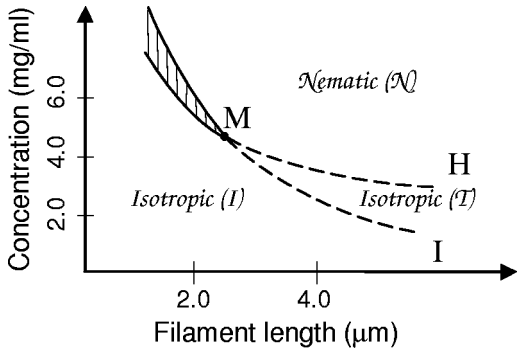

FIG. 3. Sketch of a proposed phase diagram for the *I*-*N* transition of long and stiff rods. Each phase region follows what is shown in Fig. 2 of Ref. [8], with the exception of a hatched coexistence region here. The nematic interaction (*J*) and the defect suppression (*K*) parameters of Ref. [8] are mapped to the concentration and filament length, respectively.

paramagnetic transitions. In the *I*-*N* transition situations, the more explicit order parameter corresponding to the nematic interaction *J* labeled on the ordinate in Fig. 2 of Ref. [8] is $1/T$ for a thermotropic *I*-*N* transition. In our system of a rodlike suspension, it is concentration, *c*. The defect core energy, *K*, on the abscissa in Fig. 2 of Ref. [8] translates to filament length, which scales with the defect energy of a nematic rodlike suspension. We stress here that our proposed phase diagram is only a sketch. The very existance of the proposed *I*-*T* transition, the critical point *M* and the functional forms for both the *N*-*T* and the *I*-*T* branches all call for theoretical analysis more specifically catered for rodlike suspensions and also, of course, more extensive experimental tests.

We now briefly discuss two other features that affect the *I*-*N* transition: the filament flexibility and the polydispersity of length. The flexibility is known to suppress the concentration gap between coexisting *I*-*N* domains. For instance, such a gap for the *I*-*N* transition of the semiflexible fd or *M*13 viruses is reduced to about 10% of the concentration of the coexisting isotropic phase [4], down from over 30% predicted by the Onsager theory for rigid rods [5]. The fd or *M*13 virus has about the same diameter as *F*-actin, but a persistence length of 2.2 μm [4], much shorter than that of *F*-actin (15–20 μm) [17]. Therefore, the semiflexible nature of *F*-actin is insufficient to cause the disappearance of the concentration gap characteristic of a first order transition for most polymer liquid crystals [18]. While polydispersity has been speculated as a possible cause of smearing the *I*-*N* phase boundary, calculations for bidispersed rods suggest not narrower but wider coexisting regions [19]. Experimental study of short polydisperse rods agrees [20].

Dogic and Fraden recently attempted to detect coexistence for the *I*-*N* transition of pf1, another filamentous bacteriophage of 2 μm length. Similar to our findings for the long *F*-actin, they observed no domain separation for the *I*-*N* transition (private communications). Since the pf1 virus has similar diameter and persistent length to fd or *M*13, but is twice as long, the different behavior between their *I*-*N* transitions implies that even the 2 μm filaments are perhaps too long to lead to domain separation. The similar behavior of pf1 to *F*-actin also supports the argument that polydispersity is unlikely to account for the observed continuous transition for *F*-actin, since pf1 viruses are monodisperse.

In summary, the *I*-*N* transition for *F*-actin of $l \geqslant 3$ μm is continuous in alignment and protein concentration. This experimental finding, and more importantly, its proposed relevance to the LRT theory, will likely provoke further query, such as a search for the *I*-*T* transition closely related to the *T*-*N* transition and the resultant critical fluctuations.

We acknowledge helpful discussions with Bob Pelcovits, John Toner, James Swihart, Seth Fraden, and Zvonimir Dogic. This work was supported by NSF DMR 9988389. Jorge Viamontes was supported by the U.S. Department of Education.

[1] T. Sato, Y. Jinbo, and A. Teramoto, Macromolecules **30**, 590 (1997).
[2] R.E. Buxbaum *et al.*, Science **235**, 1511 (1987).
[3] A. Kerst *et al.*, Proc. Natl. Acad. Sci. U.S.A. **87**, 4241 (1990).
[4] J.X. Tang and S. Fraden, Liq. Cryst. **19**, 459 (1995).
[5] L. Onsager, Ann. N.Y. Acad. Sci. **51**, 627 (1949).
[6] S. Chandrasekher, *Liquid Crystals* (Cambridge University Press, Cambridge, 1992).
[7] P.G. de Gennes and J. Prost, *The Physics of Liquid Crystals* (Clarendon, Oxford, 1994).
[8] P.E. Lammert, D.S. Rokhsar, and J. Toner, Phys. Rev. Lett. **70**, 1650 (1993); Phys. Rev. E **52**, 1778 (1995).
[9] J. Kas *et al.*, Biophys. J. **70**, 609 (1995).
[10] C. Coppin and P. Leavis, Biophys. J. **63**, 794 (1992).
[11] R. Furukawa, R. Kundra, and M. Fechheimer, Biochemistry **32**, 12 346 (1993).
[12] A. Suzuki, T. Maeda, and T. Ito, Biophys. J. **59**, 25 (1991).
[13] R. Oldenbourg and G. Mei, J. Microsc. **180**, 140 (1995).
[14] S. Chandrasekhar and G.S. Ranganath, Adv. Phys. **35**, 507 (1986).
[15] J.X. Tang *et al.*, Biophys. J. **76**, 2208 (1999).
[16] S.D. Lee and R.B. Meyer, J. Chem. Phys. **84**, 3443 (1986).
[17] F. Gittes *et al.*, J. Cell Biol. **120**, 923 (1993).
[18] *Polymer Liquid Crystals* edited by A. Ciferri, W.R. Krigbaum, and R.B. Meyer (Academic Press, New York, 1982).
[19] G.L. Vroege and H.N.M. Lekkerkerker, J. Phys. Chem. **97**, 3601 (1993).
[20] J. Buitenhuis *et al.*, J. Colloid Interface Sci. **175**, 46 (1995).